Theoretical models of electron spin resonance spectra

M. KAMTA[1] and S. DOMNGANG[2]

[1] *Université de Ngaoundéré, B.P. 455, ENSAI. Ngaoundéré, Cameroun.*

[2] *Université de Yaoundé I, B.P. 812, Yaoundé, Cameroun.*

RÉSUMÉ

Les modèles théoriques élaborés dans cet article ont permis d'évaluer précisément et simultanément, 20 paramètres de l'Hamiltonien de spin électronique des défauts dans le phosphure d'indium dopé au fer (InP:Fe), irradié aux électrons de 16 MeV, à l'aide d'un micro-ordinateur PC. L'algorithme d'ajustement consiste à minimiser les écarts quadratiques entre un spectre expérimental et son modèle théorique, jusqu'à ce qu'un minimum de 10^{-20} soit obtenu. Ce modèle théorique est un ensemble de fonctions multiparamétriques qui décrivent la symétrie locale d'un centre paramagnétique. Cette nouvelle méthode d'analyse des données RPE, basée sur la symétrie locale d'un centre paramagnétique, permet d'identifier des structures inconnues. Par ailleurs, elle permet de suivre le comportement des défauts pendant les traitements thermiques post-implantation requis pour contrôler l'activation électrique des atomes implantés dans un matériau substrat.

Mot clés: $I_nP:F_e$, RPE, défaut d'irradiation.

ABSTRACT

The theoretical models elaborated in this paper have enabled us to accurately and simultaneously evaluate, 20 electronic spin Hamiltonian parameters of defects in 16 MeV electron-irradiated iron-doped indium phosphide (InP:Fe), using a micro computer PC. The fitting algorithm consists in minimizing the quadratic differences between an experimental spectrum and its theoretical model, until a minimum of 10^{-20} is obtained. This theoretical model is a set of multiparametric functions, which describe the local symmetry of a paramagnetic center. This new ESR data analysis method, based on the local symmetry of a paramagnetic center, allows one to identify the unknown features. Furthermore, it allows one to monitor the behavior of the defects during the post-implantation thermal treatments required to control the electrical activation of the implanted atoms in a substrate material.

Key words: $I_nP:F_e$, ESR, radiation defects

Introduction

The use of semi-insulating materials for electronic devices requires a detailed knowledge of their behavior during usual processing techniques, such as the ion implantation reported by Favennec (1993), and its associated thermal treatments. In fact, the thermal treatments for removing particle-induced defects and for achieving the electrical activation of the implanted atoms are well monitored if these defects are identified.

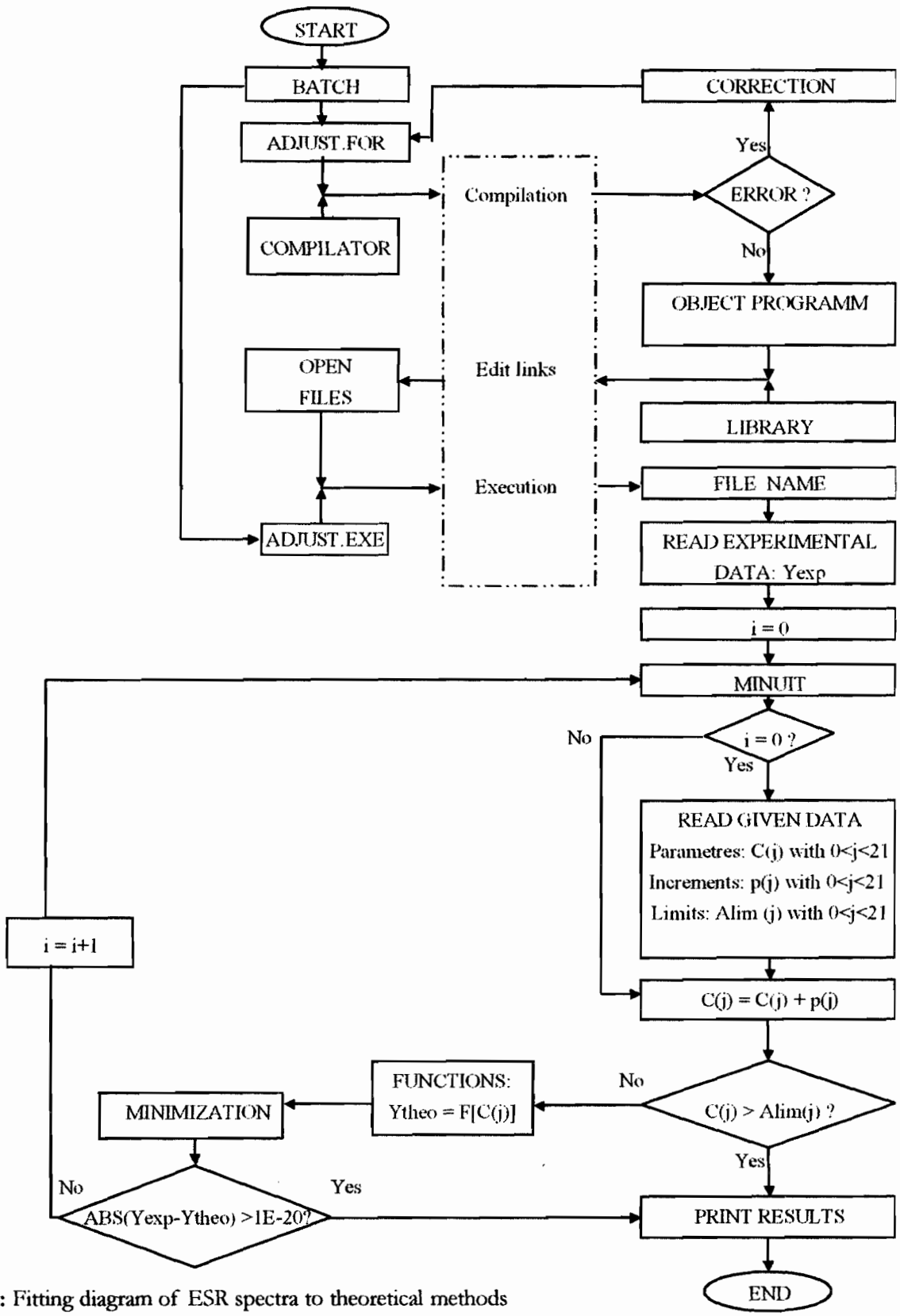

Fig. 1: Fitting diagram of ESR spectra to theoretical methods

Among the magnetic resonance techniques, electron spin resonance (ESR) is the most common one for the identification of paramagnetic centers in bulk materials. However, in III-V semi-insulating materials, the ESR lines are not resolved because of the large line-width due to interaction of the d-electrons with the nuclear spin of atoms. Furthermore, Kamta ***et al.*** (1998) have reported on electron irradiated iron-doped indium phosphide that the ESR spectra of radiation defects overlapped for particular directions of the static magnetic field, (e.g. H // [001]). Therefore, the identification of paramagnetic centers in such a material requires a very well elaborated analytical method.

Usually, the spin Hamiltonian parameters of defects in the semi-insulating materials are determined by several computer diagonalization and fittings, as reported by Nistor ***et al.*** (1997). Unfortunately, this analytical approach has failed in the case of several overlapped ESR lines.

In this paper, a new analytical method of ESR spectra is elaborated, for the paramagnetic centers of well-known local symmetry. The corresponding theoretical models are the multiparametric functions that enable one to separate several intertwining ESR lines. Therefore, the ESR parameters of several defects should accurately and simultaneously be determined.

Approach and definitions

The quantitative analysis of complex ESR spectra is done using a minimization program, the so called "MINUIT" (CERN PROGRAM LIBRARY OFFICE. CERN-CN DIVISION, CH-1211 Geneva 23, Switzerland). This program in FORTRAN searches the minima of a given multi-parametric function and analyses its shape in the vicinity of these minima.

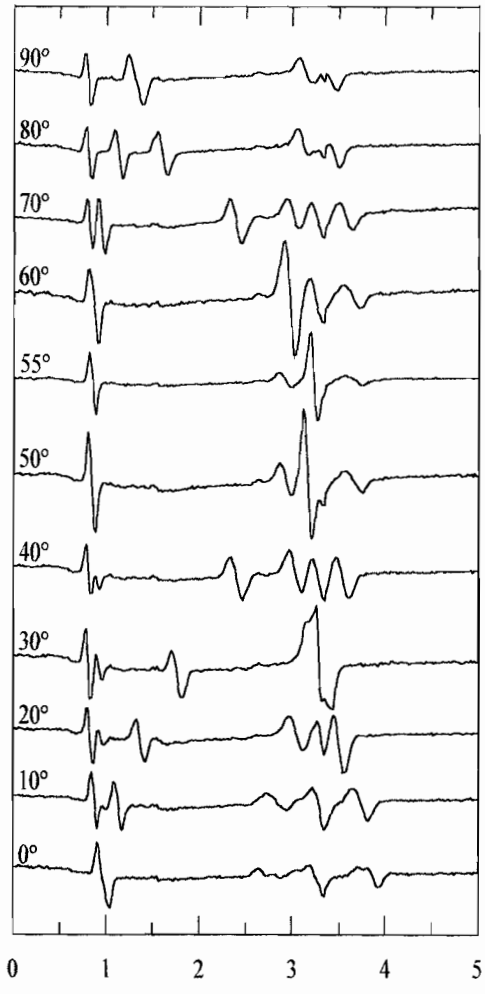

Fig.2. Angular dependence of the ESR spectrum of 16 MeV electron-irradiated SI InP:Fe in the $(1\bar{1}\,0)$ crystal plane. T = 4.2 K, P = 1 mW, 9.28 GHz.

The sub-programs have been written in accordance with the diagram sketched by Fig.1, for the whole figures in this paper. For the ESR lines close to a gaussian shape, the multi-parametric function is the first-derivative gaussian, as given by J. E. Wertz and J. R. Bolton (1972)

$$Y' = -2\ln 2 \times Y_{max}\left[\frac{Hr - H(\theta)}{\Delta H^2}\right] exp\left[-\ln 2 \frac{[Hr - H(\theta)]^2}{\Delta H^2}\right] \quad (1)$$

Y_{max} is the peak amplitude.

ΔH is the half-width at half-height.

H_r is the magnetic field at which the resonance condition is met.

$H(\theta)$ is the magnetic field in a direction θ with respect to the symmetry axis of defect.

Since the defect is in a cubic crystal (e.g., the semi-insulating InP:Fe), the directions [001], [010] and [100] are all equivalent.

The 9 GHz ESR spectra were recorded in the dark, at 4.2 K, using a rectangular TE_{102} cavity and a finger-type helium immersion cryostat. Fig. 2 shows the angular dependence of the ESR spectrum for a sample rotating in the $(1\bar{1}\ 0)$ crystal plane. Whereas many bands are split by the rotation of the sample in the $(1\bar{1}\ 0)$ crystal plane, this still leaves several unresolved features. The spectrum attributed to the Fe_{In} ($3d^5$) ion in cubic symmetry, as first reported by Stauss, ***et al.*** (1977) is observed. Furthermore, the spectrum attributed to the Fe_{In}-$In_{i,In}$ pair in trigonal symmetry, as reported by Kennedy and Wilsey (1981) is observed too.

These spectra taken at different angles in the $(1\bar{1}\ 0)$ plane were fitted to the theoretical models elaborated in this paper. The principle of the analysis was to allow for as many individual Gaussian lines as needed to remove all structures from a smooth baseline. Each Gaussian was defined by a set of three independent parameters, corresponding to its amplitude, width and position. The fitting procedure was carried out in an interactive way, by first fitting the baseline to a polynomial function, and then, the strongest and the weakest lines to the Gaussian functions. The aim of this procedure was to avoid artifacts. So, it should be possible to determine the experimental resonance positions, and to plot them as a function of rotation about a crystalline axis. Therefore, one could monitor the angular variation of the experimental resonance positions, for the magnetic field rotating in the $(1\bar{1}\ 0)$ crystal plane. As a result, the local symmetry of paramagnetic center could be shown, and the corresponding electronic spin Hamiltonian could be expressed.

Solutions

Theoretical model for a paramagnetic center of cubic symmetry.

The Landé g factor is isotropic. The electronic spin Hamiltonian were given by Abragam ***et al.*** (1970).

$$H_c = g\beta H_z S_z + \frac{a}{6}[S_\xi^4 + S_\eta^4 + S_\zeta^4 - \frac{1}{5} S(S+1)(3S^2+3S-1)] \quad (2)$$

The first term of the second member of eq.2 represents the Zeeman interaction and the second, the fine structure term due to a crystalline field of cubic symmetry.

For an ion $3d^5$ (L = 0 and S = 5/2) in a crystalline field of cubic symmetry, the 5S fine structure lines are not isotropic. So, for a diagonalized Zeeman term, Bleaney ***et al.***(1953), Matarrese ***et al.***(1956), Chihiro ***et al.*** (1960) and De Wit ***et al.*** (1963) had shown that the crystalline potential (second term of eq.2) could be expressed in terms of spherical harmonics Y_{4m} :

$$V_F = \frac{a}{120}\sum_{m=-4}^{4} F_m(\theta) Y_{4m} \quad (3)$$

where 4 is the degree and m, the order of the spherical harmonic. θ is the angle between the magnetic field and the quaternary [001] axis. $F_m(\theta)$ ($-4 \le m \le 4$) are the associated Legendre polynomials. Form eqs. (2) and (3), the (2S+1) Zeeman levels of the fundamental state $^6S_{5/2}$ were calculated, and the results can be expressed as :

$$\begin{aligned} E_{\pm 5/2} &= \pm\frac{5}{2}g\beta H + \frac{a}{8}\alpha_o \pm \frac{a^2}{g\beta H}\alpha_5 \\ E_{\pm 3/2} &= \pm\frac{3}{2}g\beta H - \frac{3a}{8}\alpha_o \pm \frac{a^2}{g\beta H}\alpha_3 \\ E_{\pm 1/2} &= \pm\frac{1}{2}g\beta H + \frac{2a}{8}\alpha_o \pm \frac{a^2}{g\beta H}\alpha_1 \end{aligned} \quad (4)$$

Where α_0, α_1, α_3 and α_5 are the angular factors :

$$\alpha_o = 15\cos^2(\theta) - 10\cos(\theta) - 1$$

$$\alpha_1 = \frac{5}{768}(3600\cos^8(\theta) - 4800\cos^6(\theta) + 544\cos^4(\theta) + 704\cos^2(\theta) - 48)$$
$$\alpha_3 = \frac{5}{768}(-2025\cos^8(\theta) + 2700\cos^6(\theta) - 342\cos^4(\theta) - 372\cos^2(\theta) + 87) \quad (5)$$
$$\alpha_5 = \frac{5}{768}(-1017\cos^8(\theta) + 1356\cos^6(\theta) - 374\cos^4(\theta) - 52\cos^2(\theta) + 135)$$

The magnetic dipolar transitions occur when :

$$h\nu = E_M - E_{M-1} \quad (6)$$

where h is the Plank's constant and ν, the microwave frequency.

Therefore, the theoretical resonance positions for an ion $3d^5$ (L = 0 and S = 5/2) in a crystalline field of cubic symmetry is deduced from eqs. (4) and (6) :

$$H_{5/2}(\theta) = \frac{1}{2g\beta_o}\left[(\nu - \frac{a\alpha_o}{2}) + \sqrt{(\nu - \frac{a\alpha_o}{2})_2 - 4a_2(\alpha_5 - \alpha_3)}\right]$$
$$H_{3/2}(\theta) = \frac{1}{2g\beta_o}\left[(\nu + \frac{5a\alpha_o}{8}) + \sqrt{(\nu + \frac{5a\alpha_o}{8})_2 - 4a_2(\alpha_3 - \alpha_1)}\right]$$
$$H_{1/2}(\theta) = \frac{1}{2g\beta_o}\left[\nu + \sqrt{\nu^2 - 8a^2\alpha_1}\right]$$
$$H_{-1/2}(\theta) = \frac{1}{2g\beta_o}\left[(\nu - \frac{5a\alpha_o}{8}) + \sqrt{(\nu - \frac{5a\alpha_o}{8})_2 - 4a_2(\alpha_3 - \alpha_1)}\right] \quad (7)$$
$$H_{-3/2}(\theta) = \frac{1}{2g\beta_o}\left[(\nu + \frac{a\alpha_o}{2}) + \sqrt{(\nu + \frac{a\alpha_o}{2})_2 - 4a_2(\alpha_5 - \alpha_3)}\right]$$

$\beta_o = \beta/h = 1.3996\ 10^9\ (s.kG)^{-1}$.

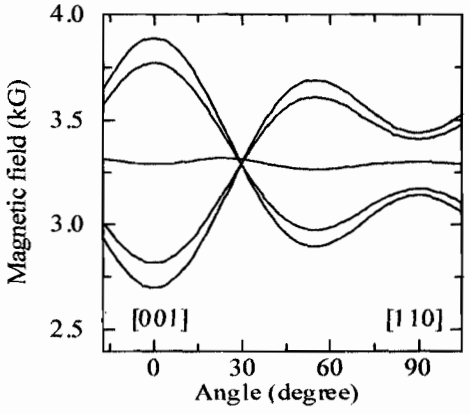

Fig.3: Rotation pattern of the theoretical resonance positions or a paramagnetic center of cubic symmetry.

Fig.3 is an illustration of theoretical model $H_M(\theta)$ for a paramagnetic center of cubic symmetry, with g = 2.002, a = 224×10^{-4} cm^{-1}, ν = 9.28 GHz, $\beta_0 = \beta / h = 1.3996\times10^9$ $(s.kG)^{-1}$.

The above parameters are typical for a neutral iron atom substituted at an In site in InP:Fe, (i.e., Fe_{In}^0 in electrical notation).

Theoretical model for a paramagnetic center of axial symmetry.

The Landé g factor is not isotropic. The electronic spin Hamiltonian were given by Abragam ***et al.*** (1970).

$$H_a = \beta[g_{//}H_zS_z + g_\perp(H_xS_x + H_yS_y)] + D[S_z^2 - S(S+1)/3] \quad (8)$$

The first term of the second member of eq.8 represents the Zeeman interaction and the second, the fine structure term due to a crystalline field of axial symmetry. The indexes z, x and y represent the quantum axes and its perpendiculars, respectively. The coefficient D is the zero field splitting factor. $g_{//}$ and $g_\perp$ are the g factors appropriate to the orientations $H_{//}$ and $H_\perp$ of the magnetic field when it is respectively parallel and perpendicular to the symmetry axis of defect. For an unperturbed paramagnetic center, assuming that D is greater than $h\nu$, the electronic spin Hamiltonian of eq. 8 is reduced to the Zeeman term. Therefore, the shape of the curves $H_i(\theta)$ is given by:

$$H_i(\theta) = \frac{\nu}{g_i(\theta)\beta_o} \qquad \text{where } i = 1, 2, 3 \qquad (9)$$

Centers of trigonal symmetry.

The g factor which reflects the trigonal symmetry is given by :

$$g_1^2(\theta) = g_{//}^2\cos^2(54.6\text{-}\theta) + g_\perp^2\sin^2(54.6\text{-}\theta)$$
$$g_2^2(\theta) = g_{//}^2\cos^2(54.6\text{+}\theta) + g_\perp^2\sin^2(54.6\text{+}\theta) \qquad (10)$$
$$g_3^2(\theta) = g_{//}^2\cos^2(54.6)\cos^2(\theta) + g_\perp^2(1\text{-}\cos^2(54.6)\cos^2(\theta))$$

From eqs. (9) and (10), the theoretical resonance positions are deduced.

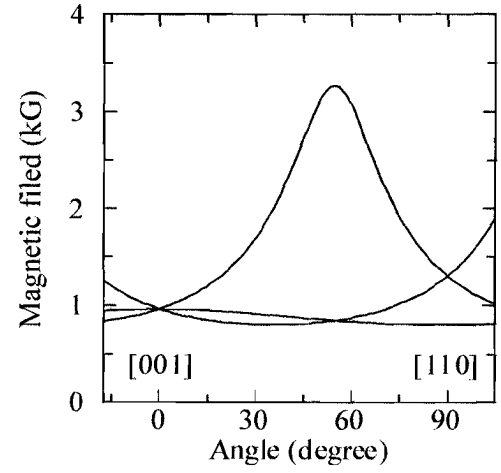

Fig.4: Rotation pattern of the theoretical resonance positions for a paramagnetic center of trigonal symmetry.

Fig. 4 is an illustration of theoretical model $H_i(\theta)$ (with i = 1, 2, 3), for a paramagnetic center of trigonal symmetry, with $g_{//} = 2.047$, $g_\perp = 8.276$. Its symmetry axis is a ternary axis [111], or its equivalents.

The above ESR parameters are typical for a pair involving the Fe_{In} atom and a nearby interstitial atom in a T_d-site, at the center of a cation tetrahedron-denoted $In_{i,In}$, for InP:Fe. This pair has been labeled Fe_{In}-$In_{i,In}$ by Kennedy and Wilsey (1981).

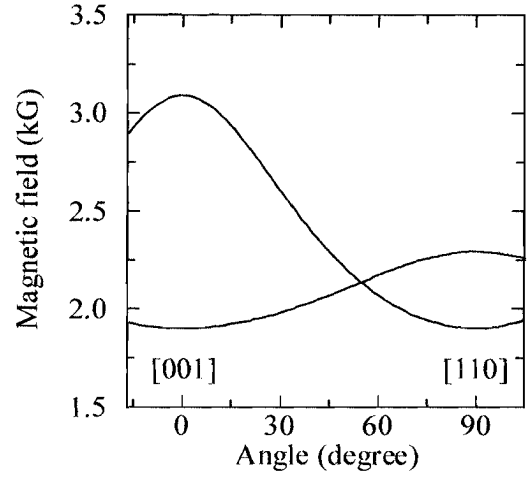

Fig.5: Rotation pattern of the theoretical resonance positions for paramagnetic center of tetragonal symmetry.

For the following theoretical resonance positions, the ESR parameters have been chosen, considering the results reported on 16 MeV electron-irradiated InP:Fe by Kamta ***et al.*** (1998).

Centers of tetragonal symmetry.

The g factor which reflects the tetragonal symmetry is given by :

$$g_1^2(\theta) = g_{//}^2\cos^2(\theta) + g_\perp\sin^2(\theta)$$
$$g_2^2(\theta) = g_{//}^2\cos^2(45)\sin^2(\theta) + g_\perp^2[1\text{-}\cos^2(45)\sin^2(\theta)] \qquad (11)$$

From eqs. (9) and (11), the theoretical resonance positions are deduced.

Fig.5 is an illustration of theoretical model $H_i(\theta)$ (with i = 1, 2), for a paramagnetic center of tetragonal symmetry, with $g_{//} = 2.25$, $g_\perp = 3.52$. Its symmetry axis is a quaternary axis [001], or its equivalents.

Centers of second order perturbed trigonal symmetry.

In the case where the Zeeman term of eq.(8) is greater than the term due to crystalline field, the later term being considered as a perturbation, the resonant field at which the allowed conditions occur were evaluated by Abragam and Bleaney (1970) :

$h\nu = g\beta H + 16\delta_1 - 8\delta_2 + \varepsilon_3$ (12) where

(δ_1, δ_2) and ε_3 are the second order perturbed terms due to an axial and a cubic crystalline field respectively. With a good accuracy, the term ε_3 can be neglected. Therefore, the terms δ_1, δ_2 are expressed by :

$$\delta_1 = \frac{D^2}{g\beta H}\cos^2(\alpha)\sin^2(\alpha)$$

$$\delta_2 = \frac{D^2}{4g\beta H}\sin^4(\alpha) \qquad (13)$$

here, α is the angle between the magnetic field and the ternary axis [111]. From the eqs. (12) and (13), the shape of the curves $H_i(\alpha)$ (where i = 1, 2, 3) is given by :

$$H_i(\alpha) = \frac{1}{2g_i(\alpha)\beta_o}\left[\nu + \sqrt{\nu^2 - 8D^2\sin^2(\alpha)\left[8\cos^2(\alpha) - \sin^2(\alpha)\right]}\right] \qquad (14)$$

The $g_i(\alpha)$ factor is given by eq.10, where α is replaced by 54.6 - θ, 54.6 + θ and θ for the following values of i : 1, 2 and 3, respectively.

Fig.6 is an illustration of theoretical model $H_i(\theta)$ (with i = 1, 2, 3), for a paramagnetic center of second order perturbed trigonal symmetry, with $g_{//} = 2.564$, $g_\perp = 4.827$ and $D = 403\times10^{-4}$ cm^{-1}.

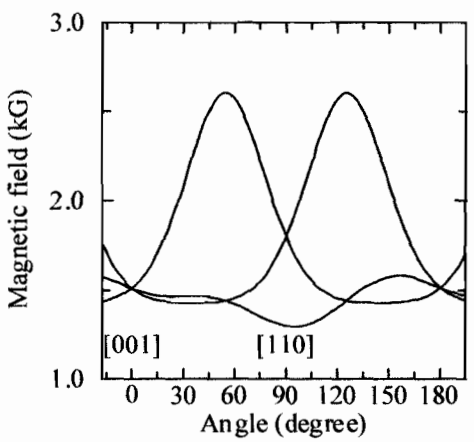

Fig.6: Rotation pattern of the theoretical resonance positions for a paramagnetic center of second order perturbed terigonal symmetry.

Centers of second order perturbed tetragonal symmetry.

The shape of the curves $H_i(\alpha)$ (where i = 1, 2) is given by eq.14. The $g_i(\alpha)$ factor is given by eq.11, where α is replaced by θ.

Fig.7 is an illustration of theoretical model $H_i(\theta)$ (with i = 1, 2), for a paramagnetic center of second order perturbed tetragonal symmetry, with $g_{//} = 2.25$, $g_\perp = 3.52$ and $D = 493\times10^{-4}$ cm^{-1}.

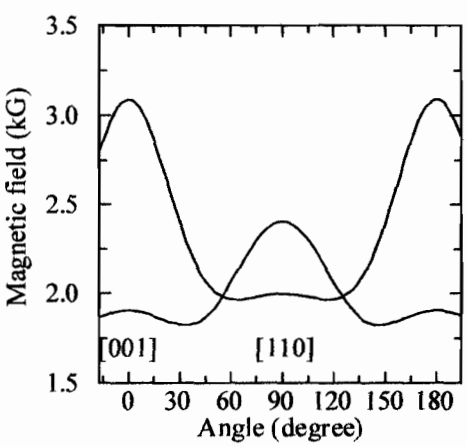

Fig.7: Rotation pattern of the theoretical resonance positions for a paramagnetic center of second order perturbed tetragonal symmetry.

Theoretical model for a paramagnetic center of orthorhombic symmetry.

The Landé g factor is not isotropic. Gehlhoff *et al.* (1990) have suggested that the spin Hamiltonian could be expressed by :

$$H_o = \beta[g_z H_z S_z + g_x H_x S_x + g_y H_y S_y)] + D[S_z^2 - S(S+1)/3] + E(S_x^2 - S_y^2) \quad (15)$$

If $2(D^2 + 3E^2)^{1/2}$ is very greater than $h\nu$, then, the allowed transitions occur between the |+1/2> and |-1/2> states. The shape of the curves $H_i(\theta)$ (where i = 1, 2, 3, 4) is given by eq.9. The effective g' factor which reflects the orthorhombic symmetry is given by :

$$g'^2_1(\theta) = g'^2_z\cos^2(\alpha-\theta) + g'^2_x\sin^2(\alpha-\theta)$$
$$g'^2_2(\theta) = g'^2_z\cos^2(\alpha+\theta) + g'^2_y\sin^2(\alpha+\theta) \quad (16)$$
$$g'^2_3(\theta) = g'^2_z\cos^2(45)\sin^2(\alpha-\theta) + g'^2_x(1- \cos^2(45)\sin^2(\alpha-\theta))$$
$$g'^2_4(\theta) = g'^2_z\cos^2(45)\sin^2(\alpha+\theta) + g'^2_x(1- \cos^2(45)\sin^2(\alpha+\theta))$$

where α is a slight deviation of the symmetry axis of defect with respect to crystalline axes. This distortion of the local symmetry of the paramagnetic centers is attributable to the particle irradiation.

Gehlhoff *et al.* (1990) have expressed the g' factor in terms the Landé g factor, for S = 3/2 :

$$g_x' = g_x\left(\pm 1 + \frac{1+3\lambda}{\sqrt{1+3\lambda^2}}\right)$$

$$g_y' = g_y\left(\pm 1 + \frac{2}{\sqrt{1+3\lambda^2}}\right) \qquad \text{with } \lambda = E/D \quad (17)$$

$$g_z' = g_z\left(1 \pm \frac{1-3\lambda}{\sqrt{1+3\lambda^2}}\right)$$

D and E are the fine structure parameters of axial and orthorhombic symmetries, respectively.

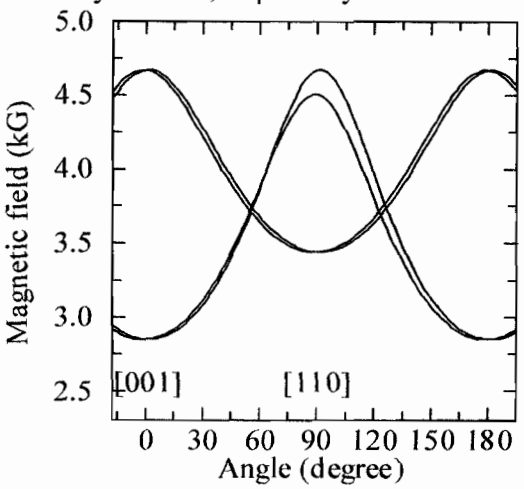

Fig.8: Rotation pattern of the theoretical resonance positions for a paramagnetic center of orthohombic symmetry.

Fig.8 is an illustration of theoretical model $H_i(\theta)$ (with i = 1, 2,3,4), for a paramagnetic center of orthorhombic symmetry, with g'_z=2.338, g'_x=1.425, g'_y=1.475, E/D=0.29.

Discussion

The ESR parameters are determined in minimizing the quadratic differences between an experimental spectrum and its theoretical spectrum defined by a multi-parametric $H(\theta)$ function. The starting parameters of $H(\theta)$ are given before running the program "MINUIT". For a particular direction of magnetic field, where most of the ESR lines are not overlapped, the constant parameters such as the Landé g factor, the fine and hyperfine structure constants, (i.e. : D(cm^{-1}) and A(cm^{-1}) respectively), are fitted to experimental data. Once these ESR constant parameters are determined with a good accuracy, they are constrained during the following fits. Then, the free parameters such as : the half-width at half-height $\Delta H(G)$ and the peak amplitude Y_{max}, are fitted, according to the diagram of Fig.1. These parameters enable one to identify a paramagnetic center. For example, the five lines fine structure attributed to Fe_{In} ($3d^5$) in cubic symmetry have to be in a ratio of : 8, 5, 9, 5, 8.

Fig.9 is an illustration of the fitting procedure elaborated in this work. The upper plot (a) shows the experimental data after cavity baseline subtraction. Curve (b) is the theoretical models of electron spin resonance spectra of cubic and trigonal symmetries respectively. Curve (c) is the error trace, which is almost flat at the

vicinity of 3.2 kG. On the other hand, the error trace is not flat at low magnetic field. In fact, the ESR lines at low magnetic field are narrow, and the baseline needs to be fitted to a polynomial of high degree.

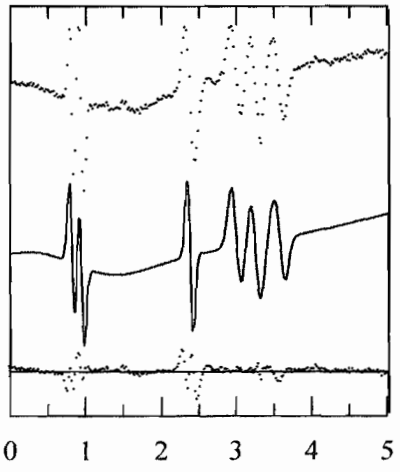

Fig.9: Illustration of the fitting of ESR spectra to the theoretical models. (a) : experimental data; (b) : sum of theoretical spectra of cubic and trigonal symmetries respectively; (c) : error trace.

Systematic use of the theoretical models of ESR spectra elaborated in this work results in rotation patterns as those shown in Fig.10. The rotation patterns of the experimental resonance positions are very closed to the rotation patterns of theoretical resonance positions.

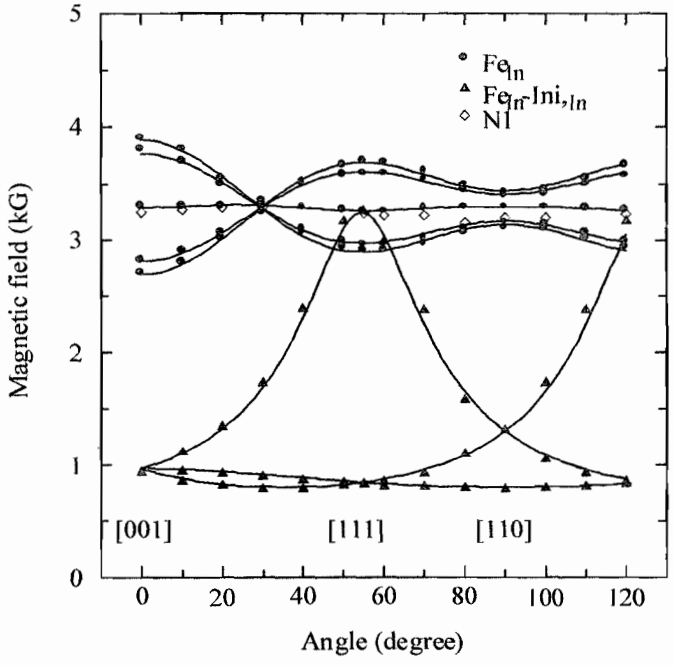

Fig.10: Rotation pattern of the individual Gaussians as derived from the fit of the ESR spectra of 16 MeV electron-irradiated InP:Fe and corresponding modelings (solid lines).

Indeed, the resulting ESR parameters are in good agreement with those reported by Stauss (1977) and Kennedy (1978) on the paramagnetic centers of cubic and trigonal symmetries respectively. The new ESR data analysis method, based on the local symmetry of a paramagnetic center, allows one to identify the unknown features, whether they are resolved or not.

References

ABRAGAM A., and Bleaney B. ***Electron Paramagnetic Resonance of Transition ions.*** (1970). (Clarendon Press. Oxford), 437.

BLEANEY B., and STEVENS K. W. H., (1953). Repts. Progr. Phys. **16**, 108.

CHIHIRO KIKUCHI and MATARRESE L. M., (1960). J. Chem. Phys. **33**, (2), 601.

CN/ASD Group, MINUIT Users Guide, Program Library D506 CERN.

De WIT M. and ESTLE T. L. (1963). Phys. Rev. **132**, (1), 195.

FAVENNEC P.-N., (1993). ***L'implantation ionique***. Masson, Paris.

GEHLHOFF W., EMANUELSON P. OMLING P., GRIMMEISS H. G., (1990). Phys. Rev. **B41**, 8560.

J. E. WERTZ, J. R. Bolton, ***Electron Spin Resonance: Elementary Theory and Practical Applications***, (McGraw-Hill, New York, 1972), 308.

KAMTA M., Schwab C., DOMNGANG S., Engel J. P., (1998). J. Appl. Phys. **84**, 4273.

KENNEDY T. A. and WILSEY N. D., (1978). Phys. Rev. Lett. **41** (4), 977.

KENNEDY T. A. and WILSEY N. D., ***Defects and Radiation Effects in Semi-conductors,*** Inst. Phys. Conf. Series n°59 (IOP, Bristol, 1981), 257.

MATARRESE L. M., and CHIHIRO KIKUCHI, (1956). J. Phys. Chem. Solids. **1**, 117-127.

NISTOR S. V., LAZAR D. P., Käβ H. and SCHOEMAKER D. (1997). Solid State Communications, **104**, 521-525.

STAUSS G. H, Krebs J. J., and HENRY R. L., (1977). Phys. Rev. **B16**, 974.

Received 04/02/2002
Accepted 22/08/2002